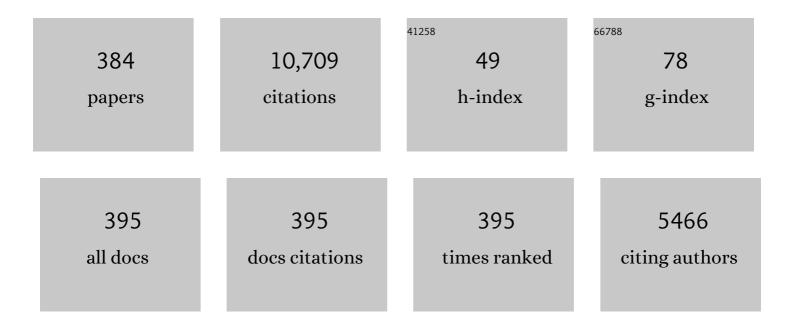
Christof Schulz

List of Publications by Year in descending order

Source: https://exaly.com/author-pdf/5688128/publications.pdf Version: 2024-02-01



#	Article	IF	CITATIONS
1	In-cylinder thermographic PIV combined with phosphor thermometry using ZnO:Zn. International Journal of Engine Research, 2023, 24, 113-131.	1.4	2
2	Synthesis of freestanding few-layer graphene in microwave plasma: The role of oxygen. Carbon, 2022, 186, 560-573.	5.4	27
3	In situ measurement of gas-borne silicon nanoparticle volume fraction and temperature by spatially and spectrally line-resolved attenuation and emission imaging. Powder Technology, 2022, 396, 535-541.	2.1	6
4	Molecular Emissions from Stretched Excitation-Pulse in Nanosecond Phase-Selective Laser-Induced Breakdown Spectroscopy of TiO ₂ Nanoaerosols. Applied Spectroscopy, 2022, , 000370282110725.	1.2	2
5	Shock-tube study of the influence of oxygenated additives on benzene pyrolysis: Measurement of optical densities, soot inception times and comparison with simulations. Combustion and Flame, 2022, 243, 111985.	2.8	5
6	A Compact Fiber-Coupled NIR/MIR Laser Absorption Instrument for the Simultaneous Measurement of Gas-Phase Temperature and CO, CO2, and H2O Concentration. Sensors, 2022, 22, 1286.	2.1	1
7	Laser-induced incandescence for non-soot nanoparticles: recent trends and current challenges. Applied Physics B: Lasers and Optics, 2022, 128, 72.	1.1	21
8	Investigating spray flames for nanoparticle synthesis via tomographic imaging using multi-simultaneous measurements (TIMes) of emission. Optics Express, 2022, 30, 15524.	1.7	9
9	Structure–activity correlation in aerobic cyclohexene oxidation and peroxide decomposition over Co _{<i>x</i>} Fe _{3â^'<i>x</i>} O ₄ spinel oxides. Catalysis Science and Technology, 2022, 12, 3594-3605.	2.1	4
10	LES of nanoparticle synthesis in the spraysyn burner: A comparison against experiments. Powder Technology, 2022, 404, 117466.	2.1	11
11	Shock tube study of the pyrolysis kinetics of Di- and trimethoxy methane. Combustion and Flame, 2022, 242, 112186.	2.8	3
12	Early particle formation and evolution in iron-doped flames. Combustion and Flame, 2022, 244, 112251.	2.8	8
13	Large-scale synthesis of iron oxide/graphene hybrid materials as highly efficient photo-Fenton catalyst for water remediation. Environmental Technology and Innovation, 2021, 21, 101239.	3.0	29
14	Experimental and numerical investigation of iron-doped flames: FeO formation and impact on flame temperature. Proceedings of the Combustion Institute, 2021, 38, 1249-1257.	2.4	20
15	Ethanol ignition in a high-pressure shock tube: Ignition delay time and high-repetition-rate imaging measurements. Proceedings of the Combustion Institute, 2021, 38, 901-909.	2.4	14
16	Thermochemistry of organosilane compounds and organosilyl radicals. Proceedings of the Combustion Institute, 2021, 38, 1259-1267.	2.4	6
17	Investigation of the combustion of iron pentacarbonyl and the formation of key intermediates in iron oxide synthesis flames. Chemical Engineering Science, 2021, 230, 116169.	1.9	9
18	Numerical Investigation of Remote Ignition in Shock Tubes. Flow, Turbulence and Combustion, 2021, 106, 471-498.	1.4	7

#	Article	IF	CITATIONS
19	Pyrolysis of diethyl carbonate: Shock-tube and flow-reactor measurements and modeling. Proceedings of the Combustion Institute, 2021, 38, 987-996.	2.4	10
20	Spray-flame synthesis of LaMO3 (M = Mn, Fe, Co) perovskite nanomaterials: Effect of spray droplet size and esterification on particle size distribution. Proceedings of the Combustion Institute, 2021, 38, 1279-1287.	2.4	19
21	Plug-flow reactor and shock-tube study of the oxidation of very fuel-rich natural gas/DME/O2 mixtures. Combustion and Flame, 2021, 225, 86-103.	2.8	21
22	Determination of gas-phase absorption cross-sections of FeO in a shock tube using intracavity absorption spectroscopy near 611†nm. Proceedings of the Combustion Institute, 2021, 38, 1637-1645.	2.4	8
23	Kinetics of the Thermal Decomposition of Ethylsilane: Shock-Tube and Modeling Study. Energy & Fuels, 2021, 35, 3266-3282.	2.5	5
24	Multi-line SiO fluorescence imaging in the flame synthesis of silica nanoparticles from SiCl4. Combustion and Flame, 2021, 224, 260-272.	2.8	12
25	Virtual Special Issue of Recent Advances in Gas-Phase Synthesis of Functional Materials for Energy. Energy & Fuels, 2021, 35, 6341-6343.	2.5	2
26	Spatial distribution of gas-phase synthesized germanium nanoparticle volume-fraction and temperature using combined in situ line-of-sight emission and extinction spectroscopy. Optics Express, 2021, 29, 8387.	1.7	10
27	Low-temperature and low-pressure effective fluorescence lifetimes and spectra of gaseous anisole and toluene. Applied Physics B: Lasers and Optics, 2021, 127, 1.	1.1	3
28	Room-temperature Fe:ZnSe laser tunable in the spectral range of 3.7–5.3â€Âµm applied for intracavity absorption spectroscopy of CO ₂ isotopes, CO and N ₂ O. Optics Express, 2021, 29, 12033.	1.7	25
29	Survivability of the thermographic phosphors YAG:Pr and SMP:Sn in a premixed flame. Measurement Science and Technology, 2021, 32, 074001.	1.4	2
30	Interrogating Gas-Borne Nanoparticles Using Laser-Based Diagnostics and Bayesian Data Fusion. Journal of Physical Chemistry C, 2021, 125, 8382-8390.	1.5	10
31	Characterization of tracers for two-color laser-induced fluorescence thermometry of liquid-phase temperature in ethanol, 2–ethylhexanoic-acid/ethanol mixtures, 1-butanol, and o-xylene. Applied Optics, 2021, 60, C98.	0.9	11
32	Crumpled few-layer graphene: Connection between morphology and optical properties. Carbon, 2021, 182, 677-690.	5.4	9
33	Phase-sensitive detection of gas-borne Si nanoparticles via line-of-sight UV/VIS attenuation. Optics Express, 2021, 29, 21795.	1.7	6
34	Atmospheric-pressure particle mass spectrometer for investigating particle growth in spray flames. Journal of Aerosol Science, 2021, 158, 105827.	1.8	16
35	Near-threshold soot formation in premixed flames at elevated pressure. Carbon, 2021, 181, 143-154.	5.4	9
36	Thermochemistry of Oxygen-Containing Organosilane Radicals and Uncertainty Estimations of Organosilane Group-Additivity Values. Journal of Physical Chemistry A, 2021, 125, 8699-8711.	1.1	2

#	Article	IF	CITATIONS
37	Experimental Investigation of Ethanol Oxidation and Development of a Reduced Reaction Mechanism for a Wide Temperature Range. Energy & Fuels, 2021, 35, 14780-14792.	2.5	14
38	Liquidâ€Phase Cyclohexene Oxidation with O ₂ over Sprayâ€Flameâ€5ynthesized La _{1â^'<i>x</i>} Sr _{<i>x</i>} CoO ₃ Perovskite Nanoparticles. Chemistry - A European Journal, 2021, 27, 16912-16923.	1.7	10
39	Simultaneous measurement of liquid-film thickness and solute concentration of aqueous solutions of two urea derivatives using NIR absorption. Applied Optics, 2021, 60, 10087.	0.9	3
40	Intracavity Absorption Spectroscopy of CO2, CO and N2O Using a Fe:ZnSe Laser Tunable in the Range of 3.7–5.3 µm. , 2021, , .		1
41	Sprayâ€flame synthesis of La(Fe, Co)O ₃ nanoâ€perovskites from metal nitrates. AICHE Journal, 2020, 66, e16748.	1.8	41
42	An experimental and modeling study on the reactivity of extremely fuel-rich methane/dimethyl ether mixtures. Combustion and Flame, 2020, 212, 107-122.	2.8	44
43	Gas-phase synthesis of iron oxide nanoparticles for improved magnetic hyperthermia performance. Journal of Alloys and Compounds, 2020, 824, 153814.	2.8	31
44	Self-assembled nano-silicon/graphite hybrid embedded in a conductive polyaniline matrix for the performance enhancement of industrial applicable lithium-ion battery anodes. Solid State Ionics, 2020, 344, 115117.	1.3	16
45	A six-compound, high performance gasoline surrogate for internal combustion engines: Experimental and numerical study of autoignition using high-pressure shock tubes. Fuel, 2020, 261, 116439.	3.4	11
46	Monitoring formaldehyde in a shock tube with a fast dual-comb spectrometer operating in the spectral range of 1740–1790Âcm–1. Applied Physics B: Lasers and Optics, 2020, 126, 1.	1.1	11
47	Laser-based CO concentration and temperature measurements in high-pressure shock-tube studies of n-heptane partial oxidation. Applied Physics B: Lasers and Optics, 2020, 126, 1.	1.1	16
48	Studying the influence of single droplets on fuel/air ignition in a high-pressure shock tube. Review of Scientific Instruments, 2020, 91, 105107.	0.6	5
49	A group additivity methodology for predicting the thermochemistry of oxygenâ€eontaining organosilanes. International Journal of Chemical Kinetics, 2020, 52, 918-932.	1.0	7
50	Flexible energy conversion and storage via high-temperature gas-phase reactions: The piston engine as a polygeneration reactor. Renewable and Sustainable Energy Reviews, 2020, 133, 110264.	8.2	31
51	Characterization of few-layer graphene aerosols by laser-induced incandescence. Carbon, 2020, 167, 870-880.	5.4	20
52	CO-concentration and temperature measurements in reacting CH4/O2 mixtures doped with diethyl ether behind reflected shock waves. Combustion and Flame, 2020, 216, 194-205.	2.8	16
53	Selective cyclohexene oxidation with O ₂ , H ₂ O ₂ and <i>tert</i> -butyl hydroperoxide over spray-flame synthesized LaCo _{1a^x} Fe _x O ₃ nanoparticles. Catalysis Science and Technology, 2020, 10, 5196-5206.	2.1	28
54	Characterization of tracers for two-color laser-induced fluorescence liquid-phase temperature imaging in sprays. Experiments in Fluids, 2020, 61, 1.	1.1	23

#	Article	IF	CITATIONS
55	Impact of shock-tube facility-dependent effects on incident- and reflected-shock conditions over a wide range of pressures and Mach numbers. Combustion and Flame, 2020, 217, 200-211.	2.8	46
56	Sprayâ€Flameâ€Prepared LaCo _{1–<i>x</i>} Fe _x O ₃ Perovskite Nanoparticles as Active OER Catalysts: Influence of Fe Content and Lowâ€Temperature Heating. ChemElectroChem, 2020, 7, 2564-2574.	1.7	21
57	High-pressure shock-tube study of the ignition and product formation of fuel-rich dimethoxymethane (DMM)/air and CH4/DMM/air mixtures. Combustion and Flame, 2020, 216, 293-299.	2.8	19
58	Shock-tube study of the decomposition of octamethylcyclotetrasiloxane and hexamethylcyclotrisiloxane. Zeitschrift Fur Physikalische Chemie, 2020, 234, 1395-1426.	1.4	6
59	Characterization of tracers for two-color laser-induced fluorescence liquid-phase temperature imaging in sprays. , 2020, , .		0
60	High-temperature gas-phase kinetics of the thermal decomposition of tetramethoxysilane. Proceedings of the Combustion Institute, 2019, 37, 1133-1141.	2.4	10
61	Gas-phase synthesis of functional nanomaterials: Challenges to kinetics, diagnostics, and process development. Proceedings of the Combustion Institute, 2019, 37, 83-108.	2.4	92
62	Comparative study of flame-based SiO2 nanoparticle synthesis from TMS and HMDSO: SiO-LIF concentration measurement and detailed simulation. Proceedings of the Combustion Institute, 2019, 37, 1221-1229.	2.4	22
63	The influence of hydrogen and methane on the growth of carbon particles during acetylene pyrolysis in a burnt-gas flow reactor. Proceedings of the Combustion Institute, 2019, 37, 1125-1132.	2.4	12
64	Shock-tube study of the ignition and product formation of fuel-rich CH4/air and CH4/additive/air mixtures at high pressure. Proceedings of the Combustion Institute, 2019, 37, 5705-5713.	2.4	23
65	Shock-tube study of methane pyrolysis in the context of energy-storage processes. Proceedings of the Combustion Institute, 2019, 37, 197-204.	2.4	32
66	Detailed simulation of iron oxide nanoparticle forming flames: Buoyancy and probe effects. Proceedings of the Combustion Institute, 2019, 37, 1241-1248.	2.4	20
67	Towards Mechanistic Understanding of Liquidâ€Phase Cinnamyl Alcohol Oxidation with tert â€Butyl Hydroperoxide over Nobleâ€Metalâ€Free LaCo 1– x Fe x O 3 Perovskites. ChemPlusChem, 2019, 84, 1155-1163	1.3	29
68	High-Temperature Unimolecular Decomposition of Diethyl Ether: Shock-Tube and Theory Studies. Journal of Physical Chemistry A, 2019, 123, 6813-6827.	1.1	12
69	Investigating temporal variation in the apparent volume fraction measured by time-resolved laser-induced incandescence. Applied Physics B: Lasers and Optics, 2019, 125, 1.	1.1	13
70	SpraySyn—A standardized burner configuration for nanoparticle synthesis in spray flames. Review of Scientific Instruments, 2019, 90, 085108.	0.6	89
71	Development and evaluation of a chemical kinetics reaction mechanism for tetramethylsilane-doped flames. Chemical Engineering Science, 2019, 209, 115209.	1.9	16
72	Absolute SiO concentration imaging in low-pressure nanoparticle-synthesis flames via laser-induced fluorescence. Applied Physics B: Lasers and Optics, 2019, 125, 1.	1.1	12

#	Article	IF	CITATIONS
73	Evaluation of Drude parameters for liquid Germanium nanoparticles through aerosol-based line-of-sight attenuation measurements. Journal of Quantitative Spectroscopy and Radiative Transfer, 2019, 226, 146-156.	1.1	4
74	Detector calibration and measurement issues in multi-color time-resolved laser-induced incandescence. Applied Physics B: Lasers and Optics, 2019, 125, 1.	1.1	12
75	Excitation wavelength dependence of the fluorescence lifetime of anisole. Physical Chemistry Chemical Physics, 2019, 21, 14562-14570.	1.3	2
76	Two-dimensional-three-dimensional registration for fusion imaging is noninferior to three-dimensional- three-dimensional registration in infrarenal endovascular aneurysm repair. Journal of Vascular Surgery, 2019, 70, 2005-2013.	0.6	14
77	Fuel effects on NO formation in diesel-like jets in a vessel. Combustion and Flame, 2019, 206, 201-210.	2.8	1
78	Power and syngas production from partial oxidation of fuel-rich methane/DME mixtures in an HCCI engine. Fuel, 2019, 243, 97-103.	3.4	45
79	The influence of selected aromatic fluorescence tracers on the combustion kinetics of iso-octane. Fuel, 2019, 244, 559-568.	3.4	5
80	Sprayâ€Flameâ€Synthesized LaCo 1â^' x Fe x O 3 Perovskite Nanoparticles as Electrocatalysts for Water and Ethanol Oxidation. ChemElectroChem, 2019, 6, 4266-4274.	1.7	28
81	Structures of carbonaceous nanoparticles formed in various pyrolysis systems. Carbon, 2019, 150, 244-258.	5.4	4
82	Synthesis of silicon nanoparticles in a pilot-plant-scale microwave plasma reactor: Impact of flow rates and precursor concentration on the nanoparticle size and aggregation. Powder Technology, 2019, 342, 880-886.	2.1	25
83	Spontaneous-Raman-scattering measurements in diesel-like n-heptane jets: Spectroscopy and flame structure. Fuel, 2019, 236, 1356-1365.	3.4	3
84	Mixing processes in the transonic, accelerated wake of a central injector. Physics of Fluids, 2019, 31, .	1.6	3
85	Laser spectroscopic investigation of diesel-like jet structure using C8 oxygenates as the fuel. Fuel, 2019, 235, 1515-1529.	3.4	10
86	Durability study of platinum nanoparticles supported on gas-phase synthesized graphene in oxygen reduction reaction conditions. Applied Surface Science, 2019, 467-468, 1181-1186.	3.1	29
87	A Cr ⁴⁺ :forsterite laser for intracavity absorption spectroscopy in the spectral range of 12–14 µm. Optics Express, 2019, 27, 11122.	1.7	11
88	NIR sensor for aqueous urea solution film thickness and concentration measurement using a broadband light source. Applied Optics, 2019, 58, 4546.	0.9	7
89	All gas-phase synthesis of graphene: Characterization and its utilization for silicon-based lithium-ion batteries. Electrochimica Acta, 2018, 272, 52-59.	2.6	40
90	LIISim: a modular signal processing toolbox for laser-induced incandescence measurements. Applied Physics B: Lasers and Optics, 2018, 124, 1.	1.1	16

#	Article	IF	CITATIONS
91	Temperature, pressure, and oxygen quenching behavior of fluorescence spectra and lifetimes of gas-phase o-xylene and 1,2,4-trimethylbenzene. Applied Physics B: Lasers and Optics, 2018, 124, 1.	1.1	3
92	Conflict-free railway track assignment at depots. Journal of Rail Transport Planning and Management, 2018, 8, 16-28.	0.8	3
93	Shock-tube study of the decomposition of tetramethylsilane using gas chromatography and high-repetition-rate time-of-flight mass spectrometry. Physical Chemistry Chemical Physics, 2018, 20, 10686-10696.	1.3	13
94	Combined production of power and syngas in an internal combustion engine – Experiments and simulations in SI and HCCI mode. Fuel, 2018, 215, 40-45.	3.4	61
95	Highâ€Temperature Rate Constants for H + Tetramethylsilane and H + Silane and Implications about Structure–Activity Relationships for Silanes. International Journal of Chemical Kinetics, 2018, 50, 57-72.	1.0	16
96	Electrostatic Self-Assembly Enabling Integrated Bulk and Interfacial Sodium Storage in 3D Titania-Graphene Hybrid. Nano Letters, 2018, 18, 336-346.	4.5	40
97	Quantitative nitrogen oxide measurements by laser-induced fluorescence in diesel-like n-heptane jets with enhanced premixing. Combustion and Flame, 2018, 188, 250-261.	2.8	11
98	Soot formation in shock-wave-induced pyrolysis of acetylene and benzene with H2, O2, and CH4 addition. Combustion and Flame, 2018, 198, 158-168.	2.8	24
99	Experimental Investigation of the Influence of the Pressure Gradient on the Transonic Mixing Behavior in Blunt-Body Wakes using Tracer LIF. , 2018, , .		2
100	Numerical Investigation of Transonic Mixing Behavior in the Wake of a Central Injector at different Reynolds numbers. , 2018, , .		1
101	Direct Measurement of High-Temperature Rate Constants of the Thermal Decomposition of Dimethoxymethane, a Shock Tube and Modeling Study. Journal of Physical Chemistry A, 2018, 122, 7559-7571.	1.1	21
102	Methodology for the investigation of ignition near hot surfaces in a high-pressure shock tube. Review of Scientific Instruments, 2018, 89, 055111.	0.6	2
103	High-Temperature Rate Constants for the Reaction of Hydrogen Atoms with Tetramethoxysilane and Reactivity Analogies between Silanes and Oxygenated Hydrocarbons. Journal of Physical Chemistry A, 2018, 122, 5289-5298.	1.1	8
104	Response surface and group additivity methodology for estimation of thermodynamic properties of organosilanes. International Journal of Chemical Kinetics, 2018, 50, 681-690.	1.0	16
105	Application of toluene LIF to transonic nozzle flows to identify zones of incomplete molecular mixing. Optics Express, 2018, 26, 10266.	1.7	6
106	Water film thickness imaging based on time-multiplexed near-infrared absorption. Optics Express, 2018, 26, 20902.	1.7	15
107	Water Film Thickness Imaging based on Time-Multiplexed Near-Infrared Absorption. , 2018, , .		0
108	Strategy for determining absolute concentration levels of SiO in low pressure gas phase synthesis flames for silica nanoparticles. , 2018, , .		0

#	Article	IF	CITATIONS
109	Parasitic Reactions in Nanosized Silicon Anodes for Lithium-Ion Batteries. Nano Letters, 2017, 17, 1512-1519.	4.5	122
110	Micrometer-sized nano-structured silicon/carbon composites for lithium-ion battery anodes synthesized based on a three-step Hansen solubility parameter (HSP) concept. Journal of Industrial and Engineering Chemistry, 2017, 52, 305-313.	2.9	10
111	SiO multi-line laser-induced fluorescence for quantitative temperature imaging in flame-synthesis of nanoparticles. Applied Physics B: Lasers and Optics, 2017, 123, 1.	1.1	16
112	UV absorption and fluorescence properties of gas-phase p-difluorobenzene. Applied Physics B: Lasers and Optics, 2017, 123, 1.	1.1	8
113	Reaction-time-resolved measurements of laser-induced fluorescence in a shock tube with a single laser pulse. Review of Scientific Instruments, 2017, 88, 115105.	0.6	6
114	A Shock Tube and Modeling Study about Anisole Pyrolysis Using Time-Resolved CO Absorption Measurements. International Journal of Chemical Kinetics, 2017, 49, 656-667.	1.0	15
115	Flame-temperature, light-attenuation, and CO measurements by spontaneous Raman scattering in non-sooting diesel-like jets. Combustion and Flame, 2017, 176, 104-116.	2.8	15
116	Experimental and numerical study of a HMDSO-seeded premixed laminar low-pressure flame for SiO2 nanoparticle synthesis. Proceedings of the Combustion Institute, 2017, 36, 1045-1053.	2.4	27
117	Spectroscopic models for laser-heated silicon and copper nanoparticles. Journal of Quantitative Spectroscopy and Radiative Transfer, 2017, 197, 3-11.	1.1	21
118	Mass spectrometric analysis of clusters and nanoparticles during the gas-phase synthesis of tungsten oxide. Proceedings of the Combustion Institute, 2017, 36, 1037-1044.	2.4	17
119	Ultraviolet absorption and laser-induced fluorescence of shock-heated acetylene. Proceedings of the Combustion Institute, 2017, 36, 4469-4475.	2.4	3
120	Self-quenching in toluene LIF. Proceedings of the Combustion Institute, 2017, 36, 4505-4514.	2.4	11
121	Ignition delay times of Jet A-1 fuel: Measurements in a high-pressure shock tube and a rapid compression machine. Proceedings of the Combustion Institute, 2017, 36, 3695-3703.	2.4	24
122	Optical properties and pyrolysis of shock-heated gas-phase anisole. Proceedings of the Combustion Institute, 2017, 36, 4525-4532.	2.4	27
123	A quantum chemical and kinetics modeling study on the autoignition mechanism of diethyl ether. Proceedings of the Combustion Institute, 2017, 36, 195-202.	2.4	55
124	Novel Si-CNT/polyaniline nanocomposites as Lithium-ion battery anodes for improved cycling performance. Materials Today: Proceedings, 2017, 4, S263-S268.	0.9	8
125	Performance of photomultipliers in the context of laser-induced incandescence. Applied Optics, 2017, 56, 7849.	0.9	12
126	Sequential signal detection for high dynamic range time-resolved laser-induced incandescence. Optics Express, 2017, 25, 2413.	1.7	12

#	Article	IF	CITATIONS
127	Instantaneous 3D imaging of highly turbulent flames using computed tomography of chemiluminescence. Applied Optics, 2017, 56, 7385.	0.9	70
128	Inline coating of silicon nanoparticles in a plasma reactor: Reactor design, simulation and experiment. Materials Today: Proceedings, 2017, 4, S118-S127.	0.9	13
129	Uncertainty quantification and design-of-experiment in absorption-based aqueous film parameter measurements using Bayesian inference. Applied Optics, 2017, 56, E1.	2.1	6
130	Laser-induced atomic emission of silicon nanoparticles during laser-induced heating. Applied Optics, 2017, 56, E50.	2.1	19
131	A single-pulse shock tube coupled with high-repetition-rate time-of-flight mass spectrometry and gas chromatography for high-temperature gas-phase kinetics studies. Review of Scientific Instruments, 2016, 87, 105103.	0.6	23
132	Applications of Intracavity Absorption Spectroscopy to Quantitative Gas-Phase Species and Temperature Diagnostics. , 2016, , .		0
133	Shock-tube and plug-flow reactor study of the oxidation of fuel-rich CH4/O2 mixtures enhanced with additives. Combustion and Flame, 2016, 169, 307-320.	2.8	45
134	A novel magnetically-separable porous iron-oxide nanocomposite as an adsorbent for methylene blue (MB) dye. Journal of Environmental Chemical Engineering, 2016, 4, 3779-3787.	3.3	27
135	Diode laser-based standoff absorption measurement of water film thickness in retro-reflection. Applied Physics B: Lasers and Optics, 2016, 122, 1.	1.1	8
136	Laser-induced incandescence from laser-heated silicon nanoparticles. Applied Physics B: Lasers and Optics, 2016, 122, 1.	1.1	37
137	Time-resolved detection of temperature, concentration, and pressure in a shock tube by intracavity absorption spectroscopy. Applied Physics B: Lasers and Optics, 2016, 122, 1.	1.1	22
138	Measurements of liquid film thickness, concentration, and temperature of aqueous urea solution by NIR absorption spectroscopy. Applied Physics B: Lasers and Optics, 2016, 122, 1.	1.1	20
139	Quantitative two-dimensional measurement of oil-film thickness by laser-induced fluorescence in a piston-ring model experiment. Applied Optics, 2016, 55, 269.	2.1	25
140	High-yield and scalable synthesis of a Silicon/Aminosilane-functionalized Carbon NanoTubes/Carbon (Si/A-CNT/C) composite as a high-capacity anode for lithium-ion batteries. Journal of Applied Electrochemistry, 2016, 46, 229-239.	1.5	15
141	Laser-based diagnostics in the gas-phase synthesis of inorganic nanoparticles. Powder Technology, 2016, 287, 226-238.	2.1	42
142	LASER-INDUCED INCANDESCENCE MEASUREMENTS OF SILICON AND COPPER NANOPARTICLES: SPECTROSCOPIC MODEL. , 2016, , .		1
143	DLAS-based measurement of water film thickness in retro-reflection. , 2016, , .		0
144	Laser-induced atomic emission of silicon nanoparticles during synthesis in a microwave plasma reactor. , 2016, , .		1

#	Article	IF	CITATIONS
145	Low-pressure effective fluorescence lifetimes and photo-physical rate constants of one- and two-ring aromatics. Applied Physics B: Lasers and Optics, 2015, 121, 549-558.	1.1	12
146	Measurements of liquid film thickness, concentration and temperature of aqueous NaCl solution by NIR absorption spectroscopy. Applied Physics B: Lasers and Optics, 2015, 120, 397-406.	1.1	15
147	A Genetic Algorithm–Based Method for the Optimization of Reduced Kinetics Mechanisms. International Journal of Chemical Kinetics, 2015, 47, 695-723.	1.0	36
148	Si–CNT/rGO Nanoheterostructures as Highâ€Performance Lithiumâ€lonâ€Battery Anodes. ChemElectroChem, 2015, 2, 1983-1990.	1.7	33
149	Nitric Oxide Measurements in the Core of Diesel Jets Using a Biofuel Blend. SAE International Journal of Materials and Manufacturing, 2015, 8, 458-471.	0.3	10
150	Optical Investigation of Biofuel Effects on NO and PAH Formation in Diesel-Like Jets. , 2015, , .		7
151	Initial reaction steps during flame synthesis of iron-oxide nanoparticles. CrystEngComm, 2015, 17, 6930-6939.	1.3	41
152	A Standard Burner for High Pressure Laminar Premixed Flames: Detailed Soot Diagnostics. Zeitschrift Fur Physikalische Chemie, 2015, 229, 781-805.	1.4	13
153	Impact of Ambient Pressure on Titania Nanoparticle Formation During Spray-Flame Synthesis. Journal of Nanoscience and Nanotechnology, 2015, 15, 9449-9456.	0.9	24
154	Ignition delay times of diethyl ether measured in a high-pressure shock tube and a rapid compression machine. Proceedings of the Combustion Institute, 2015, 35, 259-266.	2.4	73
155	Endoscopic temperature imaging in a four-cylinder IC engine via two-color toluene fluorescence. Proceedings of the Combustion Institute, 2015, 35, 3697-3705.	2.4	20
156	Two-tracer LIF imaging of preferential evaporation of multi-component gasoline fuel sprays under engine conditions. Proceedings of the Combustion Institute, 2015, 35, 2915-2922.	2.4	41
157	Calibration-free, high-speed, in-cylinder laser absorption sensor for cycle-resolved, absolute H2O measurements in a production IC engine. Proceedings of the Combustion Institute, 2015, 35, 3653-3661.	2.4	21
158	Influence of carbon content, particle size, and partial manganese substitution on the electrochemical performance of LiFexMn1-xPO4/carbon composites. Ionics, 2015, 21, 1857-1866.	1.2	9
159	Sensitivity analysis for soot particle size imaging with laser-induced incandescence at high pressure. Applied Physics B: Lasers and Optics, 2015, 119, 745-763.	1.1	26
160	Effect of fluctuations on time-averaged multi-line NO-LIF thermometry measurements of the gas-phase temperature. Applied Physics B: Lasers and Optics, 2015, 120, 429-440.	1.1	10
161	Determination of small soot particles in the presence of large ones from time-resolved laser-induced incandescence. Applied Physics B: Lasers and Optics, 2015, 118, 169-183.	1.1	34
162	Temporally and spectrally resolved UV absorption and laser-induced fluorescence measurements during the pyrolysis of toluene behind reflected shock waves. Applied Physics B: Lasers and Optics, 2015, 118, 295-307.	1.1	14

#	Article	IF	CITATIONS
163	Combination of LII and extinction measurements for determination of soot volume fraction and estimation of soot maturity in non-premixed laminar flames. Applied Physics B: Lasers and Optics, 2015, 119, 685-696.	1.1	38
164	Assessment of soot particle-size imaging with LII at Diesel engine conditions. Applied Physics B: Lasers and Optics, 2015, 119, 765-776.	1.1	21
165	Direct self-assembly of Fe ₂ O ₃ /reduced graphene oxide nanocomposite for high-performance lithium-ion batteries. Journal of Materials Chemistry A, 2015, 3, 11566-11574.	5.2	58
166	Laser-induced incandescence: Particulate diagnostics for combustion, atmospheric, and industrial applications. Progress in Energy and Combustion Science, 2015, 51, 2-48.	15.8	295
167	Laser-based in situ measurement and simulation of gas-phase temperature and iron atom concentration in a pilot-plant nanoparticle synthesis reactor. Proceedings of the Combustion Institute, 2015, 35, 2299-2306.	2.4	29
168	Experimental study of the kinetics of ethanol pyrolysis and oxidation behind reflected shock waves and in laminar flames. Proceedings of the Combustion Institute, 2015, 35, 393-400.	2.4	52
169	Toluene Laser-Induced Fluorescence (LIF) Imaging of Supersonic Flow within a Diverging Duct with Injectors in the Supersonic Region. , 2015, , 471-476.		1
170	Laser-Induced Incandescence (LII) Measurements on Gas-Borne Silicon Nanoparticles. , 2014, , .		0
171	Probing Species Formed by Pilot Injection During Re-Compression in a Controlled Auto-Ignition Engine by H2CO LIF and Chemiluminescence Imaging. SAE International Journal of Engines, 2014, 7, 772-789.	0.4	7
172	An automated thermophoretic soot sampling device for laboratory-scale high-pressure flames. Review of Scientific Instruments, 2014, 85, 045103.	0.6	27
173	Measurements of Liquid Film Thickness and Solute Concentration of Aqueous NaCl Solution by Absorption Spectroscopy. , 2014, , .		1
174	Formaldehyde laser-induced fluorescence imaging with a multi-band transmission filter. Optics Letters, 2014, 39, 1873.	1.7	5
175	A Genetic Algorithmâ€Based Method for the Automatic Reduction of Reaction Mechanisms. International Journal of Chemical Kinetics, 2014, 46, 41-59.	1.0	37
176	Influence of molecular hydrogen on acetylene pyrolysis: Experiment and modeling. Combustion and Flame, 2014, 161, 2263-2269.	2.8	15
177	Mixing Processes in a Compressible Accelerated Nozzle Flow with Blunt-Body Wakes. AIAA Journal, 2014, 52, 559-568.	1.5	8
178	In situ nanoparticle size measurements of gas-borne silicon nanoparticles by time-resolved laser-induced incandescence. Applied Physics B: Lasers and Optics, 2014, 116, 623-636.	1.1	62
179	Silicon/Polyaniline Nanocomposites as Anode Material for Lithium Ion Batteries. Journal of the Electrochemical Society, 2014, 161, A40-A45.	1.3	68
180	Surface functionalization of microwave plasma-synthesized silica nanoparticles for enhancing the stability of dispersions. Journal of Nanoparticle Research, 2014, 16, 1.	0.8	30

#	Article	IF	CITATIONS
181	A comparison of selected organic tracers for quantitative scalar imaging in the gas phase via laser-induced fluorescence. Applied Physics B: Lasers and Optics, 2014, 117, 183-194.	1.1	29
182	Ignition delay times of shock-heated tetraethoxysilane, hexamethyldisiloxane, and titanium tetraisopropoxide. Chemical Physics Letters, 2014, 601, 54-58.	1.2	5
183	Endoscopic Chemiluminescence Measurements as a Robust Experimental Tool in High-Pressure Gas Turbine Combustion Tests. , 2014, , .		5
184	Liquid film thickness measurement by two-line TDLAS. , 2014, , .		0
185	Spatially-resolved measurements of gas-phase temperature and SiO concentration in a low-pressure nanoparticle synthesis reactor using laser-induced fluorescence. , 2014, , .		2
186	In Situ Laser Diagnostics in the Gas-Phase Synthesis of Functional Nanomaterials. , 2014, , .		0
187	Mechanism of Iron Oxide Formation from Iron Pentacarbonylâ€Doped Lowâ€Pressure Hydrogen/Oxygen Flames. International Journal of Chemical Kinetics, 2013, 45, 487-498.	1.0	31
188	Photo-physical properties of anisole: temperature, pressure, and bath gas composition dependence of fluorescence spectra and lifetimes. Applied Physics B: Lasers and Optics, 2013, 112, 203-213.	1.1	30
189	Temperature, pressure, and bath gas composition dependence of fluorescence spectra and fluorescence lifetimes of toluene and naphthalene. Applied Physics B: Lasers and Optics, 2013, 110, 81-93.	1.1	48
190	Simultaneous measurement of localized heat-release with OH/CH2O–LIF imaging and spatially integrated OHâ^— chemiluminescence in turbulent swirl flames. Proceedings of the Combustion Institute, 2013, 34, 3549-3556.	2.4	55
191	Experimental investigation and modeling of the kinetics of CCl4 pyrolysis behind reflected shock waves using high-repetition-rate time-of-flight mass spectrometry. Physical Chemistry Chemical Physics, 2013, 15, 2821.	1.3	10
192	High-pressure shock-tube investigation of the impact of 3-pentanone on the ignition properties of primary reference fuels. Proceedings of the Combustion Institute, 2013, 34, 393-400.	2.4	14
193	Synthesis of Small Carbon Nanoparticles in a Microwave Plasma Flow Reactor. Zeitschrift Fur Physikalische Chemie, 2013, 227, 357-370.	1.4	5
194	Thermal stratification in an internal combustion engine due to wall heat transfer measured by laser-induced fluorescence. Proceedings of the Combustion Institute, 2013, 34, 2911-2919.	2.4	58
195	VCSEL-based, high-speed, in situ TDLAS for in-cylinder water vapor measurements in IC engines. Optics Express, 2013, 21, 19951.	1.7	113
196	Buoyancy induced limits for nanoparticle synthesis experiments in horizontal premixed low-pressure flat-flame reactors. Combustion Theory and Modelling, 2013, 17, 504-521.	1.0	15
197	Low temperature diffusion of Li atoms into Si nanoparticles and surfaces. Journal of Applied Physics, 2013, 114, 034310.	1.1	3
198	In Situ Particle Size Measurements of Gas-Borne Silicon Nanoparticles by Time-Resolved Laser-Induced Incandescence. , 2013, , .		0

#	Article	IF	CITATIONS
199	Thickness imaging of evaporating liquid water films by simultaneous Tracer-LIF, Raman imaging and Diode Laser Absorption Spectroscopy. , 2012, , .		0
200	Diffractive/refractive (hybrid) UV-imaging system for minimally invasive metrology: design, performance, and application experiments. Applied Optics, 2012, 51, 1982.	0.9	14
201	In-cylinder temperature measurements via time-correlated single-photon counting of toluene laser-induced fluorescence through a fiber-based sensor. Optics Letters, 2012, 37, 5244.	1.7	5
202	Comparison of Micro- and Nanoscale Fe+3–Containing (Hematite) Particles for Their Toxicological Properties in Human Lung Cells In Vitro. Toxicological Sciences, 2012, 126, 173-182.	1.4	47
203	Application of Endoscopic OH*-Chemiluminescence Measurements at a Full-Scale High-Pressure Gas Turbine Combustion Test Rig. , 2012, , .		1
204	High-speed tunable diode laser absorption spectroscopy for sampling-free in-cylinder water vapor concentration measurements in an optical IC engine. Applied Physics B: Lasers and Optics, 2012, 109, 521-532.	1.1	48
205	Experimental and modeling study of carbon suboxide decomposition behind reflected shock waves. Physical Chemistry Chemical Physics, 2012, 14, 1246-1252.	1.3	12
206	Synthesis of Tailored Nanoparticles in Flames: Chemical Kinetics, In Situ Diagnostics, Numerical Simulation, and Process Development. Nanoscience and Technology, 2012, , 3-48.	1.5	1
207	High-capacity cathodes for lithium-ion batteries from nanostructured LiFePO4 synthesized by highly-flexible and scalable flame spray pyrolysis. Journal of Power Sources, 2012, 216, 76-83.	4.0	66
208	Toluene Laser-Induced Fluorescence (LIF) Imaging of Supersonic Flow within a Diverging Duct. , 2012, , 509-514.		3
209	Nanoparticles from the Gasphase. Nanoscience and Technology, 2012, , .	1.5	14
210	Experimental and Numerical Investigation of CH* and OH* Chemiluminescence in Acetylene Combustion behind Reflected Shock Waves. , 2012, , 421-426.		1
211	Two-dimensional cycle-resolved exhaust valve temperature measurements in an optically accessible internal combustion engine using thermographic phosphors. Applied Physics B: Lasers and Optics, 2012, 106, 945-951.	1.1	37
212	Strain rate and fuel composition dependence of chemiluminescent species profiles in non-premixed counterflow flames: comparison with model results. Applied Physics B: Lasers and Optics, 2012, 107, 561-569.	1.1	6
213	Simultaneous measurement of localized heat release with OH/CH2O-LIF imaging and spatially integrated OHâ^— chemiluminescence in turbulent swirl flames. Applied Physics B: Lasers and Optics, 2012, 107, 611-617.	1.1	28
214	Investigation of the kinetics of OHâ^— and CHâ^— chemiluminescence in hydrocarbon oxidation behind reflected shock waves. Applied Physics B: Lasers and Optics, 2012, 107, 515-527.	1.1	34
215	Selected papers about chemiluminescence of flames. Applied Physics B: Lasers and Optics, 2012, 107, 513-514.	1.1	0
216	The autoignition of practical fuels at HCCI conditions: High-pressure shock tube experiments and phenomenological modeling. Fuel, 2012, 93, 492-501.	3.4	59

#	Article	IF	CITATIONS
217	On the effect of molecular and hydrocarbon-bonded hydrogen on carbon particle formation in C3O2 pyrolysis behind shock waves. Combustion and Flame, 2012, 159, 932-939.	2.8	4
218	Autoignition of surrogate biodiesel fuel (B30) at high pressures: Experimental and modeling kinetic study. Combustion and Flame, 2012, 159, 996-1008.	2.8	28
219	Stabilization of mid-sized silicon nanoparticles by functionalization with acrylic acid. Nanoscale Research Letters, 2012, 7, 76.	3.1	74
220	Visualization of the gas flow in fuel cell bipolar plates using molecular flow seeding and micro-particle image velocimetry. Experiments in Fluids, 2012, 52, 743-748.	1.1	4
221	A Shock-Tube with High-Repetition-Rate Time-of-Flight Mass Spectrometry for the Study of Complex Reaction Systems. , 2012, , 191-196.		1
222	In-cylinder temperature measurements via fiber-based toluene-LIF time-correlated single-photon counting. , 2012, , .		1
223	Functionalization of SiO2 Nanoparticles and Their Superhydrophobic Surface Coating. Special Publication - Royal Society of Chemistry, 2012, , 113-120.	0.0	0
224	High speed in-cylinder laser hygrometry for EGR quantification using a wavelength scanned vertical cavity surface emitting laser. , 2012, , .		0
225	Gas-Temperature Imaging in aÂMicrowave-Plasma Nanoparticle-Synthesis Reactor Using Multi-Line NO-LIF Thermometry. Zeitschrift Fur Physikalische Chemie, 2011, 225, 1225-1235.	1.4	12
226	Plasma synthesis of nanostructures for improved thermoelectric properties. Journal Physics D: Applied Physics, 2011, 44, 174034.	1.3	101
227	Laser-based diagnostics for the measurement of liquid water film thickness. Applied Optics, 2011, 50, A60.	2.1	17
228	Gas-Phase Synthesis of Nanoscale Silicon as an Economical Route towards Sustainable Energy Technology. KONA Powder and Particle Journal, 2011, 29, 191-207.	0.9	56
229	High temperature shock-tube study of the reaction of gallium with ammonia. Physical Chemistry Chemical Physics, 2011, 13, 4149.	1.3	6
230	Measurement of water film thickness by laser-induced fluorescence and Raman imaging. Applied Physics B: Lasers and Optics, 2011, 102, 123-132.	1.1	30
231	Imaging of the oxygen distribution in an isothermal turbulent free jet using two-color toluene LIF imaging. Applied Physics B: Lasers and Optics, 2011, 103, 707-715.	1.1	23
232	Tunable diode laser absorption sensor for the simultaneous measurement of water film thickness, liquid- and vapor-phase temperature. Applied Physics B: Lasers and Optics, 2011, 104, 21-27.	1.1	23
233	Synthesis of tailored WO3 and WOx (2.9 <x<3) 1883-1890.<="" 2011,="" 33,="" a="" adjusting="" ar="" by="" combustion="" conditions="" flame="" h2="" in="" institute,="" nanoparticles="" o2="" of="" premixed="" proceedings="" reactor.="" td="" the=""><td>2.4</td><td>21</td></x<3)>	2.4	21
234	Temperature and bath gas composition dependence of effective fluorescence lifetimes of toluene excited at 266nm. Chemical Physics, 2011, 383, 6-11.	0.9	30

#	Article	IF	CITATIONS
235	Auto-ignition of toluene-doped n-heptane and iso-octane/air mixtures: High-pressure shock-tube experiments and kinetics modeling. Combustion and Flame, 2011, 158, 172-178.	2.8	118
236	Ignition delay times of ethanol-containing multi-component gasoline surrogates: Shock-tube experiments and detailed modeling. Fuel, 2011, 90, 1238-1244.	3.4	92
237	Unburned gas temperature measurements in a surrogate Diesel jet via two-color toluene-LIF imaging. Proceedings of the Combustion Institute, 2011, 33, 783-790.	2.4	24
238	Recent Activities in Silicon Hydride Research in Europe. , 2011, , .		1
239	A shock tube with a high-repetition-rate time-of-flight mass spectrometer for investigations of complex reaction systems. Review of Scientific Instruments, 2011, 82, 084103.	0.6	30
240	Simultaneous measurement of liquid water film thickness andÂvapor temperature using near-infrared tunable diode laser spectroscopy. Applied Physics B: Lasers and Optics, 2010, 99, 385-390.	1.1	25
241	Temperature and species measurement in a quenching boundary layer on a flat-flame burner. Experiments in Fluids, 2010, 49, 783-795.	1.1	32
242	Study of the H+O+M reaction forming OHâ^—: Kinetics of OHâ^— chemiluminescence in hydrogen combustion systems. Combustion and Flame, 2010, 157, 1261-1273.	2.8	108
243	Optical diagnostics in diesel combustion engines. , 2010, , 617-643.		2
244	Measurement and Chemical Kinetics Modeling of Shock-Induced Ignition of Ethanolâ^'Air Mixtures. Energy & Fuels, 2010, 24, 2830-2840.	2.5	80
245	Advanced direct injection combustion engine technologies and development. , 2010, , .		25
246	In-Situ Laser Diagnostics of Temperature, Intermediate Species Concentration and Particle Sizes in Gas-Phase Nanoparticle Synthesis. , 2010, , .		0
247	Measurements of Liquid Film Thickness by Tracer LIF, Raman Scattering and Diode Laser Absorption Spectroscopy. , 2010, , .		0
248	Enhanced long-term stability of functionalized silicon nanoparticles using esters. Materials Research Society Symposia Proceedings, 2009, 1207, 1.	0.1	2
249	Quantitative liquid and vapor distribution measurements in evaporating fuel sprays using laser-induced exciplex fluorescence. Measurement Science and Technology, 2009, 20, 125401.	1.4	46
250	Imaging measurements of atomic iron concentration withÂlaser-induced fluorescence in a nanoparticle synthesis flame reactor. Applied Physics B: Lasers and Optics, 2009, 94, 119-125.	1.1	35
251	Investigation of toluene LIF at high pressure and high temperature in an optical engine. Applied Physics B: Lasers and Optics, 2009, 96, 735-739.	1.1	31
252	Spectroscopic characterization of the fluorobenzene/DEMA tracer system for laser-induced exciplex fluorescence for the quantitative study of evaporating fuel sprays. Applied Physics B: Lasers and Optics, 2009, 97, 909-918.	1.1	24

#	Article	IF	CITATIONS
253	Visualization of the evaporation of a diesel spray using combined Mie and Rayleigh scattering techniques. Experiments in Fluids, 2009, 47, 439-449.	1.1	24
254	Experiments and modeling of ignition delay times, flame structure and intermediate species of EHN-doped stoichiometric n-heptane/air combustion. Proceedings of the Combustion Institute, 2009, 32, 197-204.	2.4	27
255	Autoignition of gasoline surrogate mixtures at intermediate temperatures and high pressures: Experimental and numerical approaches. Proceedings of the Combustion Institute, 2009, 32, 501-508.	2.4	84
256	Electrical properties of aluminum-doped zinc oxide (AZO) nanoparticles synthesized by chemical vapor synthesis. Nanotechnology, 2009, 20, 445701.	1.3	77
257	Gas-phase synthesis of non-agglomerated nanoparticles by fast gasdynamic heating and cooling. , 2009, , 857-862.		13
258	Experimental and Numerical Investigation of Fe(CO) ₅ Addition to a Laminar Premixed Hydrogen/Oxygen/Argon Flame. Zeitschrift Fur Physikalische Chemie, 2009, 223, 639-649.	1.4	27
259	Discrepancies between shock tube and rapid compression machine ignition at low temperatures and high pressures. , 2009, , 739-744.		22
260	Shock-tube study of the ignition delay time of tetraethoxysilane (TEOS). , 2009, , 781-785.		1
261	Temperature dependence of the soot yield in shock wave pyrolysis of carbon-containing precursors. , 2009, , 183-188.		0
262	Ga2O3 nanoparticles synthesized in a low-pressure flame reactor. Journal of Nanoparticle Research, 2008, 10, 121-127.	0.8	6
263	Laser-induced incandescence for soot-particle sizing at elevated pressure. Applied Physics B: Lasers and Optics, 2008, 90, 629-639.	1.1	43
264	Toluene laser-induced fluorescence for in-cylinder temperature imaging in internal combustion engines. Applied Physics B: Lasers and Optics, 2008, 91, 669-675.	1.1	88
265	Fluorescence quantum yield of carbon dioxide for quantitative UV laser-induced fluorescence in high-pressure flames. Applied Physics B: Lasers and Optics, 2008, 93, 677-685.	1.1	9
266	Modeling laser-induced incandescence of soot: enthalpy changes during sublimation, conduction, and oxidation. Applied Physics B: Lasers and Optics, 2008, 93, 645-656.	1.1	25
267	Autoignition of gasoline surrogates mixtures at intermediate temperatures and high pressures. Combustion and Flame, 2008, 152, 276-281.	2.8	131
268	Effect of active impurities on the condensation of nanoparticles from supersaturated carbon vapor in the combined laser photolysis of C3O2 and H2S. Kinetics and Catalysis, 2008, 49, 167-177.	0.3	2
269	Development of a two-line OH-laser-induced fluorescence thermometry diagnostics strategy for gas-phase temperature measurements in engines. Applied Optics, 2008, 47, 5871.	2.1	27
270	Laser-Based Experimental and Monte Carlo PDF Numerical Investigation of an Ethanol/Air Spray Flame. Combustion Science and Technology, 2008, 180, 1529-1547.	1.2	35

#	Article	IF	CITATIONS
271	Thermal Decomposition of Trimethylgallium Ga(CH ₃) ₃ : A Shock-Tube Study and First-Principles Calculations. Journal of Physical Chemistry A, 2008, 112, 6330-6337.	1.1	17
272	Influence of the bath gas on the condensation of supersaturated iron atom vapour at room temperature. Journal Physics D: Applied Physics, 2008, 41, 055203.	1.3	42
273	Micro-invasive LIF Diagnostics in Engines. , 2008, , .		0
274	Core and grain boundary sensitivity of tungsten-oxide sensor devices by molecular beam assisted particle deposition. Journal of Applied Physics, 2007, 102, 124305.	1.1	21
275	Quantification of the evaporative cooling in an ethanol spray created by a gasoline direct-injection system measured by multiline NO-LIF gas-temperature imaging. Applied Optics, 2007, 46, 8322.	2.1	12
276	Direct-Flame Solid-Oxide Fuel Cell (DFFC): A Thermally Self-Sustained, Air Self- Breathing, Hydrocarbon-Operated SOFC System in a Simple, No-Chamber Setup. ECS Transactions, 2007, 7, 555-564.	0.3	24
277	Shock-tube study of the autoignition of n-heptane/toluene/air mixtures at intermediate temperatures and high pressures. Combustion and Flame, 2007, 149, 25-31.	2.8	115
278	Heat release of carbon particle formation from hydrogen-free precursors behind shock waves. Proceedings of the Combustion Institute, 2007, 31, 649-656.	2.4	26
279	Unsteady flame and flow field interaction of a premixed model gas turbine burner. Proceedings of the Combustion Institute, 2007, 31, 3197-3205.	2.4	26
280	Formation of carbon nanoparticles by the condensation of supersaturated atomic vapor obtained by the laser photolysis of C3O2. Kinetics and Catalysis, 2007, 48, 194-203.	0.3	11
281	Modeling laser-induced incandescence of soot: a summary and comparison of LII models. Applied Physics B: Lasers and Optics, 2007, 87, 503-521.	1.1	197
282	Gas-temperature imaging in a low-pressure flame reactor for nano-particle synthesis with multi-line NO-LIF thermometry. Applied Physics B: Lasers and Optics, 2007, 88, 373-377.	1.1	42
283	Functionalization of silicon nanoparticles via hydrosilylation with 1-alkenes. Colloid and Polymer Science, 2007, 285, 729-736.	1.0	51
284	Synthesis of SnO2â^'x nanoparticles tuned between 0⩽x⩽1 in a premixed low pressure H2/O2/Ar flame. Proceedings of the Combustion Institute, 2007, 31, 1805-1812.	2.4	21
285	Experimental and numerical characterization of a turbulent spray flame. Proceedings of the Combustion Institute, 2007, 31, 2247-2255.	2.4	51
286	A direct-flame solid oxide fuel cell (DFFC) operated on methane, propane, and butane. Journal of Power Sources, 2007, 166, 120-126.	4.0	78
287	Combustion Diagnostics. , 2007, , 1241-1315.		37
288	Temperature and Heat Flux. , 2007, , 487-561.		7

#	Article	IF	CITATIONS
289	Transport and Diffusion in Boundary Layers of Turbulent Channel Flow. , 2007, , 419-432.		0
290	Branching ratios for quenching of nitric oxide A2Σ+(ν′ = 0) to X2Î(ν″ = 0). Physical Chemistry Chemical Physics, 2006, 8, 5328-5338.	1.3	24
291	Novel strategies for imaging temperature distribution using Toluene LIF. Journal of Physics: Conference Series, 2006, 45, 133-139.	0.3	52
292	Laser-based temperature imaging close to surfaces with toluene and NO-LIF. Journal of Physics: Conference Series, 2006, 45, 69-76.	0.3	7
293	Two-color time-resolved LII applied to soot particle sizing in the cylinder of a Diesel engine. Combustion and Flame, 2006, 147, 79-92.	2.8	91
294	Fluorescence lifetime of gas-phase toluene at elevated temperatures. Chemical Physics Letters, 2006, 426, 248-251.	1.2	17
295	TR-LII for sizing of carbon particles forming at room temperature. Applied Physics B: Lasers and Optics, 2006, 83, 449-454.	1.1	30
296	Laser-Induced Incandescence. Applied Physics B: Lasers and Optics, 2006, 83, 331-331.	1.1	5
297	Laser-induced incandescence: recent trends and current questions. Applied Physics B: Lasers and Optics, 2006, 83, 333-354.	1.1	427
298	Nanoparticle formation from supersaturated carbon vapour generated by laser photolysis of carbon suboxide. Journal Physics D: Applied Physics, 2006, 39, 4359-4365.	1.3	6
299	Laser-based imaging measurements in combustion: New results for fuel/air mixture and temperature diagnostics. Journal of Physics: Conference Series, 2006, 45, 27-27.	0.3	3
300	Vibrational and defect states in SnOx nanoparticles. Journal of Applied Physics, 2006, 99, 113108.	1.1	26
301	Temperature Diagnostics Using Laser-Induced Fluorescence (LIF) of Toluene. , 2006, , .		2
302	Advanced Laser Imaging Diagnostics in Combustion. Zeitschrift Fur Physikalische Chemie, 2005, 219, 509-554.	1.4	5
303	Predicting LIF signal strength for toluene and 3-pentanone under engine-related temperature and pressure conditions. Proceedings of the Combustion Institute, 2005, 30, 1545-1553.	2.4	65
304	Numerical simulation and laser-based imaging of mixture formation, ignition, and soot formation in a diesel spray. Proceedings of the Combustion Institute, 2005, 30, 2029-2036.	2.4	19
305	Tracer-LIF diagnostics: quantitative measurement of fuel concentration, temperature and fuel/air ratio in practical combustion systems. Progress in Energy and Combustion Science, 2005, 31, 75-121.	15.8	492
306	Instantaneous three-dimensional visualization of concentration distributions in turbulent flows with crossed-plane laser-induced fluorescence imaging. Applied Physics B: Lasers and Optics, 2005, 80, 125-131.	1.1	7

#	Article	IF	CITATIONS
307	Toluene LIF at elevated temperatures: implications for fuel–air ratio measurements. Applied Physics B: Lasers and Optics, 2005, 80, 147-150.	1.1	57
308	Oxygen quenching of toluene fluorescence at elevated temperatures. Applied Physics B: Lasers and Optics, 2005, 80, 777-784.	1.1	81
309	Application of advanced laser diagnostics for the investigation of the ionization sensor signal in a combustion bomb. Applied Physics B: Lasers and Optics, 2005, 81, 1135-1142.	1.1	2
310	Gas-phase temperature imaging in spray systems using multi-line NO-LIF thermometry. Applied Physics B: Lasers and Optics, 2005, 81, 1071-1074.	1.1	25
311	Quantitative in-cylinder NO-LIF imaging in a realistic gasoline engine with spray-guided direct injection. Proceedings of the Combustion Institute, 2005, 30, 2667-2674.	2.4	33
312	Toluene Laser-Induced Fluorescence (LIF) Under Engine-Related Pressures, Temperatures and Oxygen Mole Fractions. , 2005, , .		5
313	Effects of Bio Diesel Injection in a DI Diesel Engine on Gaseous and Particulate Emission. , 2005, , .		10
314	Fiber optic spark plug sensor for UV-LIF measurements close to the ignition spark. , 2005, , .		4
315	Nonstationary Collisional Dynamics in Determining Nitric Oxide Laser-Induced Flourescence Spectra. AIAA Journal, 2005, 43, 458-464.	1.5	18
316	UV absorption of CO2 for temperature diagnostics of hydrocarbon combustion applications. Proceedings of the Combustion Institute, 2005, 30, 1591-1599.	2.4	33
317	Quantitative temperature measurements in high-pressure flames with multiline NO-LIF thermometry. Applied Optics, 2005, 44, 6718.	2.1	49
318	Measurement of the Equivalence Ratio in the Spark Gap Region of a Gasoline Direct Injection Engine With Spark Emission Spectroscopy and Tracer-LIF. , 2004, , .		5
319	Laser-induced fluorescence of tracers dissolved in evaporating droplets. Applied Physics B: Lasers and Optics, 2004, 78, 127-131.	1.1	20
320	Quantitative multi-line NO-LIF temperature imaging. Applied Physics B: Lasers and Optics, 2004, 78, 519-533.	1.1	98
321	Spray diagnostics using an all-solid-state Nd:YAlO3 laser and fluorescence tracers in commercial gasoline and diesel fuels. Applied Physics B: Lasers and Optics, 2004, 79, 249-254.	1.1	12
322	Method for absolute OH-concentration measurements in premixed flames by LIF and numerical simulations. Applied Physics B: Lasers and Optics, 2004, 79, 759-766.	1.1	6
323	UV planar laser induced fluorescence imaging of hot carbon dioxide in a high-pressure flame. Applied Physics B: Lasers and Optics, 2004, 79, 427-430.	1.1	10
324	Absorption and fluorescence of toluene vapor at elevated temperatures. Physical Chemistry Chemical Physics, 2004, 6, 2940.	1.3	140

#	Article	IF	CITATIONS
325	Carbon Dioxide UV Laser-Induced Fluorescence Imaging in High-Pressure Flames. , 2004, , .		1
326	Role of Non-Stationary Collisional Dynamics in Determining Nitric Oxide LIF Spectra. , 2004, , .		3
327	Rayleigh-calibrated fluorescence quantum yield measurements of acetone and 3-pentanone. Applied Optics, 2004, 43, 5901.	2.1	31
328	Carbon dioxide UV laser-induced fluorescence in high-pressure flames. Chemical Physics Letters, 2003, 375, 344-349.	1.2	33
329	Strategies for laser-induced fluorescence detection of nitric oxide in high-pressure flames II A–X(0,1) excitation. Applied Optics, 2003, 42, 2031.	2.1	40
330	Laser-induced incandescence for soot diagnostics at high pressures. Applied Optics, 2003, 42, 2052.	2.1	79
331	Strategies for laser-induced fluorescence detection of nitric oxide in high-pressure flames III Comparison of A–X excitation schemes. Applied Optics, 2003, 42, 4922.	2.1	68
332	Quantitative NO-LIF Temperature Imaging in High-Pressure Flames. , 2003, , .		1
333	Laser-induced fluorescence detection of no in high-pressure flames with A-X(0,0), (0,1), and (0,2) excitation. , 2002, , .		0
334	Strategies for laser-induced fluorescence detection of nitric oxide in high-pressure flames I A–Xexcitation. Applied Optics, 2002, 41, 3547.	2.1	61
335	Strategies for NO Laser-Induced Fluorescence in Methane/Air Flames at Pressures between 1 and 60 bar. , 2002, , FB4.		1
336	Quantitative NO-LIF imaging in high-pressure flames. Applied Physics B: Lasers and Optics, 2002, 75, 97-102.	1.1	57
337	Quantitative oxygen imaging in an engine. Applied Physics B: Lasers and Optics, 2002, 75, 137-141.	1.1	26
338	Oxygen-distribution imaging with a novel two-tracer laser-induced fluorescence technique. Applied Physics B: Lasers and Optics, 2002, 74, 111-114.	1.1	47
339	Detailed modeling and laser-induced fluorescence imaging of nitric oxide in a NH3-seeded non-premixed methane/air flame. Proceedings of the Combustion Institute, 2002, 29, 2195-2202.	2.4	25
340	Impact of UV absorption by CO2 and H2O on no lif inhigh-pressure combustion applications. Proceedings of the Combustion Institute, 2002, 29, 2735-2742.	2.4	48
341	Ultraviolet absorption spectra of shock-heated carbon dioxide and water between 900 and 3050 K. Chemical Physics Letters, 2002, 355, 82-88.	1.2	72
342	Two-line laser-induced fluorescence imaging of vibrational temperatures in a NO-seeded flame. Applied Optics, 2001, 40, 748.	2.1	43

#	Article	IF	CITATIONS
343	In-Cylinder Combustion Visualization in an Auto-Igniting Gasoline Engine using Fuel Tracer- and Formaldehyde-LIF Imaging. , 2001, , .		41
344	Quantitative In-Cylinder NO-LIF Imaging in a Direct-Injected Gasoline Engine with Exhaust Gas Recirculation. , 2001, , .		8
345	Measurements and simulation of in-cylinder UV-absorption in spark ignition and Diesel engines. Applied Physics B: Lasers and Optics, 2001, 73, 173-180.	1.1	31
346	Fluorescence imaging of natural gas/air mixing without tracers added. Chemical Physics Letters, 2001, 345, 259-264.	1.2	10
347	Simultaneous single-shot laser-based imaging of formaldehyde, OH, and temperature in turbulent flames. Proceedings of the Combustion Institute, 2000, 28, 279-286.	2.4	97
348	Laser diagnostic analysis of no formation in a direct injection diesel engine with pump-line-nozzle and common rail injection systems. Proceedings of the Combustion Institute, 2000, 28, 1137-1143.	2.4	29
349	Three-dimensional modeling with Monte Carlo-probability density function methods and laser diagnostics of the combustion in a two-stroke engine. Proceedings of the Combustion Institute, 2000, 28, 1153-1159.	2.4	17
350	Measurement of temperature, fuel concentration and equivalence ratio fields using tracer LIF in IC engine combustion. Applied Physics B: Lasers and Optics, 2000, 71, 717-723.	1.1	158
351	Laser-diagnostic multi-species imaging in strongly swirling natural gas flames. Applied Physics B: Lasers and Optics, 2000, 71, 741-746.	1.1	19
352	Single-shot laser-induced fluorescence imaging of formaldehyde with XeF excimer excitation. Applied Physics B: Lasers and Optics, 2000, 70, 733-735.	1.1	29
353	Flame Front Analysis in Turbulent Combustion. Informatik Aktuell, 2000, , 325-333.	0.4	5
354	In-Cylinder NO-LIF Imaging in a Realistic GDI Engine Using KrF Excimer Laser Excitation. , 1999, , .		13
355	NO-flow tagging by photodissociation of NO2. A new approach for measuring small-scale flow structures. Chemical Physics Letters, 1999, 307, 15-20.	1.2	57
356	Laser-spectroscopic investigation of OH-radical concentrations in the exhaust plane of jet engines. Geophysical Research Letters, 1999, 26, 1849-1852.	1.5	9
357	Quantification of NO A–X(0, 2) laser-induced fluorescence: investigation of calibration and collisional influences in high-pressure flames. Applied Optics, 1999, 38, 1434.	2.1	45
358	Investigation of spatially resolved light absorption in a spark-ignition engine fueled with propane/air. Applied Optics, 1999, 38, 1452.	2.1	24
359	Laser Diagnostics of Combustion Processes: From Chemical Dynamics to Technical Devices. Israel Journal of Chemistry, 1999, 39, 1-24.	1.0	19
360	Analysis of Chemical Dynamics and Technical Combustion by Time-Resolved Laser-Induced Fluorescence. , 1999, , 241-275.		0

#	Article	IF	CITATIONS
361	Comparative study of experimental and numerical no profiles in SI combustion. Proceedings of the Combustion Institute, 1998, 27, 2077-2084.	0.3	13
362	Multidimensional laser diagnostic and numerical analysis of no formation in a gasoline engine. Proceedings of the Combustion Institute, 1998, 27, 2085-2092.	0.3	15
363	Laser-diagnostic and numerical study of strongly swirling natural gas flames. Proceedings of the Combustion Institute, 1998, 27, 1023-1029.	0.3	45
364	Simultaneous Mapping of the Distribution of Different Fuel Volatility Classes Using Tracer-LIF Tomography in an IC Engine. , 1998, , .		26
365	Laser Spectroscopic Investigation of Flow Fields and NO-Formation in a Realistic SI Engine. , 1998, , .		18
366	Laser-induced-fluorescence detection of nitric oxide in high-pressure flames with A–X(0, 2) excitation. Applied Optics, 1997, 36, 3227.	2.1	59
367	Quantitative 2D single-shot imaging of no concentrations and temperatures in a transparent SI engine. Proceedings of the Combustion Institute, 1996, 26, 2597-2604.	0.3	57
368	A laser-induced fluorescence scheme for imaging nitric oxide in engines. Chemical Physics Letters, 1995, 242, 259-264.	1.2	51
369	Enhanced coalescence upon laser desorption of fullerene oxides. Journal of Chemical Physics, 1994, 101, 3243-3249.	1.2	55
370	Two-Dimensional Temperature Measurements in an SI Engine Using Two-Line Tracer LIF. , 0, , .		23
371	Application of laser diagnostics to engine combustion. , 0, , .		Ο
372	Innovative Ultra-low NOx Controlled Auto-Ignition Combustion Process for Gasoline Engines: the 4-SPACE Project. , 0, , .		128
373	Quantitative Laser Diagnostic Studies of the NO Distribution in a DI Diesel Engine with PLN and CR Injection Systems. , 0, , .		12
374	Multi-Species Laser-Based Imaging Measurements in a Diesel Spray. , 0, , .		15
375	NO Laser-Induced Fluorescence Imaging in the Combustion Chamber of a Spray-Guided Direct-Injection Gasoline Engine. , 0, , .		3
376	Hybrid Endoscopes for Laser-Based Imaging Diagnostics in IC Engines. , 0, , .		5
377	Study of Soot Formation and Oxidation in the Engine Combustion Network (ECN), Spray A: Effects of Ambient Temperature and Oxygen Concentration. SAE International Journal of Engines, 0, 6, 352-365.	0.4	38
378	Endoscopic Imaging of Early Flame Propagation in a Near-Production Engine. SAE International Journal of Engines, 0, 7, 351-365.	0.4	19

#	Article	IF	CITATIONS
379	Mixture-Formation Analysis by PLIF in an HSDI Diesel Engine Using C ₈ -Oxygenates as the Fuel. SAE International Journal of Fuels and Lubricants, 0, 8, 396-414.	0.2	6
380	Investigation of the Mixing Process and the Fuel Mass Concentration Fields for a Gasoline Direct-Injection Spray at ECN Spray G Conditions and Variants. , 0, , .		4
381	Direct rate-constant measurements and theoretical insight into the mechanism of the reactions H + hexamethyldisiloxane and H + tetramethyldisiloxane*. Molecular Physics, 0, , e1963871.	0.8	2
382	UV-Absorption Measurements by Spontaneous Raman Scattering in Low-Sooting Diesel-Like Jets. , 0, , .		1
383	Characterization of Oxygenated-Fuel Combustion by Quantitative Multiscalar SRS/LIF Measurements in a Diesel-Like Jet. , 0, , .		0
384	A New Methodology to Study the Mechanisms of Combustion-Chamber Deposit Formation and the Effects of Engine Parameters on the Quantity and Morphology of Combustion-Chamber Deposits. , 0, , .		1